Published in final edited form as:
J Orthop Res. 2013 January ; 31(1): 147–154. doi:10.1002/jor.22178.

Osteoblast and Osteocyte-Specific Loss of Connexin43 Results in Delayed Bone Formation and Healing During Murine Fracture Healing

Alayna E. Loiselle, **Emmanuel M. Paul**, **Gregory S. Lewis**, and **Henry J. Donahue**[#]
Pennsylvania State University, College of Medicine, Division of Musculoskeletal Sciences, Hershey, PA 17033

Abstract

Connexin43 (Cx43) plays an important role in osteoblastic differentiation in vitro, and bone formation in vivo. Mice with osteoblast/osteocyte specific loss of Cx43 display decreased gap junctional intercellular communication (GJIC), bone density and cortical thickness. To determine the role of Cx43 in fracture healing, a closed femur fracture was induced in Osteocalcin-Cre+; $Cx43^{flox/flox}$ (Cx43cKO) and Cre-$Cx43^{flox/flox}$ (WT) mice. We tested the hypothesis that loss of Cx43 results in decreased bone formation and impaired healing following fracture. Here we show that osteoblast and osteocyte-specific deletion of Cx43 results in decreased bone formation, bone remodeling, and mechanical properties during fracture healing. Cx43cKO mice display decreased bone volume, total volume, and fewer TRAP+ osteoclasts. Furthermore, loss of Cx43 in mature osteoblasts and osteocytes results in a significant decrease in torsional rigidity between 21 and 35 days post-fracture, compared to WT mice. These studies identify a novel role for the gap junction protein Cx43 during fracture healing, suggesting that loss of Cx43 can result in both decreased bone formation, and bone resorption. Therefore, enhancing Cx43 expression or GJIC may provide a novel means to enhance bone formation during fracture healing.

Keywords

Connexin 43; Fracture healing; Mouse model; Bone formation; Bone remodeling

Introduction

Connexin 43 (Cx43) is the most abundant gap junction protein in bone [1]. Cx43 has been shown to play many important roles in both bone formation and homeostasis including regulation of osteoblastic proliferation [2], differentiation [3-5] and survival [6]. *In vitro* work from our laboratory has shown that gap junction intercellular communication (GJIC) is required between osteocytes and osteoblasts in order to transduce biophysical signals such as fluid flow induced shear stress [7-9], while Cx43 also regulates the response to mechanical loading of bone in vivo [10, 11]. Additionally, general up-regulation of Cx43 has been observed during fracture healing in young and aged rats [12].

Connexin 43 is encoded by the *Gja1* gene, and complete loss of *Gja1* results in delayed mineralization of the skeleton and decreased osteoblastic differentiation in vitro [4]. Severe cardiac defects in $Gja1^{-/-}$ mice result in death soon after birth [13], and necessitate the use of conditional deletion constructs to study the postnatal role of Cx43 in bone function

[#]**Corresponding Author:** Penn State College of Medicine 500 University Dr. Mail Code H089 Hershey, PA 17033 717-531-4809 hdonahue@psu.edu.

including fracture healing. Mice with osteoblast/osteocyte specific (Osteocalcin-Cre) loss of Cx43 display decreased GJIC, bone density, cortical thickness and load at failure [11] consistent with an osteopenic phenotype. Cx43 deficient mice also have an altered response to mechanical loading [10, 11] and are less sensitive to the anabolic effects of PTH [14].

Fracture healing is divided in to four main over-lapping stages; inflammation, bridging cartilaginous callus formation, mineralization of callus, and bone remodeling [15]. Cx43 is expressed in cartilage [16-18], and is required for mineralization [4], and osteoclastogenesis [19], suggesting that Cx43 may play a vital role in multiple stages of fracture healing. Furthermore, Cx43 is required for the anabolic effects of parathyroid hormone (PTH) [14], which can enhance fracture healing [20]. The purpose of this study was to examine the role of Cx43 in mature osteoblasts and osteocytes during fracture healing, and test the hypothesis that loss of Cx43 results in impaired fracture healing due to decreased osteoblast differentiation and bone formation. Identification of the role of Cx43 in fracture healing may identify a novel clinical target to improve fracture healing.

Methods

Mice

All animal procedures were approved by the Penn State College of Medicine IACUC. Cx43 conditional knockout mice were generated by crossing Osteocalcin-Cre mice (provided by Dr. Tom Clemens)[21] with Cx43 flox/flox mice (provided by Dr. Roberto Civitelli)[22]. This cross resulted in loss of Cx43 expression in mature osteoblasts and osteocytes [11].

Fracture Healing Model

A closed femur fracture was induced in 10-week old female WT and Cx43cKO mice by three-point bending [23]. Fractures were stabilized with a 25g intramedullary pin. Femurs were harvested between seven and 35 days post-fracture.

Histology and TRAP staining

Fractured femurs were harvested and fixed in 10% neutral buffered formalin for three days. Following de-calcification, tissues were processed and embedded in paraffin. Five-micron sections were stained with Alcian Blue/ Hematoxylin/ Orange G or used for TRAP staining of osteoclasts. Tissue sections were stained with TRAP (tartrate resistant acid phosphatase) as previously described [24]. The number of multi-nucleated (greater than or equal to three nuclei/ per cell) TRAP+ cells was counted in a 1600×735 μm area at the mid-point of the callus for each specimen. Three sections per specimen were analyzed, with five-micron sections analyzed from three depths of the tissue that were approximately 35μm apart. The data are presented as mean TRAP+ osteoclasts/area ± SEM.

Immunohistochemistry

Paraffin sections were de-waxed, dehydrated, and underwent antigen retrieval using sodium citrate buffer (pH 6.0). Sections were probed with anti-Cx43 antibody (Sigma #SAB4300504), or anti-β-Galactosidase antibody (Invitrogen #A11132) diluted 1:500 in normal goat serum, followed by goat anti-rabbit secondary antibody (VectaStain), and staining was visualized with DAB chromogen (Invitrogen). Sections were counterstained with Methyl Green. Negative control sections underwent the same procedure but were probed with anti-rabbit IgG (Cell Signaling # 3900S) at 1:500.

Histomorphometry

The total tissue area of the callus was measured in NIH Image J (http://rsbweb.nih.gov/ij/), the areas of mineralized tissue (excluding cortical bone), and cartilage (as assessed by Alcian blue staining) were then measured. Three sections per specimen were analyzed, with five-micron sections analyzed from three depths of the tissue that were approximately 35μm apart. Three specimens per genotype/ time-point were analyzed. The relative proportions of mineralized and cartilaginous tissue are expressed as a percentage of the total tissue area.

Micro computed tomography

Following harvest, specimens were scanned with a VivaCT 40 Scanner (Scanco Medical AG, Brüttisellen, Switzerland) at high resolution with a voxel size of 10.5 μM. The reconstructed images were segmented and analyzed using the Image Processing Library supplied by the manufacturer. MicroCT analysis was completed by selecting the approximate slice of fracture, and reconstructing 50 slices proximal and distal to this slice, resulting in a 100-slice segment of bone for analysis. Bone volume, total volume, BV/TV, and low density bone volume were calculated by semi-manually segmenting axial slices to include the callus, and exclude cortical bone and the medullary cavity. Specimens were analyzed at thresholds of 200 and 300. A threshold of 200 included high and low-density mineralized tissue, and calcified cartilage, but excluded soft tissue and non-calcified cartilage. A threshold of 300 included only high-density mineralized tissue. To account for changes in bone modeling/ remodeling activity during healing, we used low-density bone volume as an indicator of the relative activity of healing. Bone volume at 300 was subtracted from bone volume at 200, resulting in total low-density bone volume. An increased amount of low-density bone indicates more actively remodeling bone. Total callus volume included all tissue including mineralized and un-mineralized tissue.

Biomechanical Torsion Testing

Following harvest, and removal of intramedullary pins, specimens were potted in to square aluminum pots using PMMA (poly [methyl-meth-acrylate]), rehydrated in phosphate buffered saline and tested in torsion at a rate of 1°/sec until failure using a 177N-mm load cell. Torsional rigidity was calculated as the slope of the linear region of the curve of rotational deformation (Radians) normalized to gage length (mm), versus torque (N*mm).

Statistical Analysis

A two-way Analysis of Variance (ANOVA) followed by a Bonferonni's post-test was used to determine significant differences with respect to both genotype and time post-fracture.

Results

Cx43 is widely expressed in the fracture callus

Cx43 is expressed in the fracture callus between 10 and 35 days (Figure 1A-E). Cx43 was expressed in osteoblasts lining areas of new bone formation (white arrows) between 10 and 28 days post-fracture (Figure 1A-D). Cx43 was also expressed in osteocytes (yellow arrow, Figure 2C), chondrocytes (yellow arrow, Figure 1A) and marrow cells (yellow arrow, Figure 1D). By 35 days post-fracture, a lack of Cx43-positive cells were observed in the newly formed bone (blue arrow, Figure 1E).

To assess the temporal-spatial pattern of Cre recombinase, tissue sections from Cx43cKO fractures were probed with anti-β-galactosidase antibody because a LacZ reporter gene follows the 'floxed' Cx43 DNA [22]. Following Cre mediated recombination, and excision of Cx43, expression of LacZ occurs. β-galactosidase expression was observed in osteoblasts

lining newly formed bone (white arrows, supplemental Figure 1A-D), and osteocytes (blue arrows, supplemental Figures 1A-D), showing a similar expression pattern to Cx43 in WT fractures (Figure 1).

Cx43cKO fractures heal with decreased mineralization

A bridging cartilaginous callus was formed in WT and Cx43cKO by 10 days post-fracture (Figure 2A&B). By 14 days, cartilage was present in both genotypes (Figure 2C&D); however, there was a larger area of cartilage in Cx43cKO fractures compared to WT (Figure 2K, p=0.0062), while WT fractures had a greater proportion of mineralized tissue compared to Cx43cKO (Figure 2L, p=0.0133). Small islands of mineralized tissue (blue arrow, Figure 2E) were present in WT fractures at 21 days, while cortical bone, which had not been remodeled (black arrows, Figure 2F), at the fracture site is still present in Cx43cKO fractures. Additionally, Cx43cKO maintained a significantly increased area of cartilaginous tissue (Figure 2K, p=0.0052) compared to WT at 21 days. By 28 days post-fracture, larger areas of mineralized tissue were present in the WT callus (Figure 2G, blue arrows), with a significant increase in the proportion of mineralized tissue compared to Cx43cKO (Figure 2H and L, p=0.0215), while minimal areas of mineralized tissue were present in Cx43cKO fractures and cortical bone remained un-remodeled (Figure 2H, black arrows). Cortical bridging and remodeling of the callus occurred in both WT and Cx43cKO by 35 days with no differences in mineralized tissue (Figure 2I, J and L). In addition to an increased area of cartilage in the Cx43cKO fractures at 14 and 21 days (Figure 2K), there was also persistent alcian blue staining of cartilage in the callus of Cx43cKO fractures at 28 days (Supplemental Figure 2D), while alcian blue staining was not present in WT fractures at this time (Supplemental Figure 2C).

Decreased TRAP+ osteoclasts in the callus of Cx43cKO fractures

Significant decreases in TRAP+ osteoclasts were observed in Cx43cKO fractures, relative to WT, on day 14 (Figure 3A&B, Table S1), 21 (Figure 3C&D, Table S1) and 28 (Table S1). At 14 days post-fracture there was a significantly increased number of TRAP+, multi-nucleated osteoclasts in WT fractures, compared to Cx43cKO fractures. By 21 days post-fracture, the number of TRAP+ osteoclasts decreased in both groups, with a further decrease at 28 days. By day 35 TRAP+ osteoclast number had decreased to the lowest number in each group, however, there was no significant difference between WT and Cx43cKO fractures at this time-point.

Callus bone volume and total callus volume are decreased in Cx43cKO fractures

Three-dimensional microCT images reveal that WT and Cx43cKO both formed an initial callus by 14 days post-fracture. In WT mice there was progressive remodeling of the callus through 35 days resulting in a gradual decrease in callus size (Figure 4A-D). Cx43cKO fractures follow a similar pattern of healing, with extensive remodeling of the callus by 35 days as well (Figure 4E-H). Callus bone volume (BV) was significantly increased at 14 days post-fracture in WT compared to Cx43cKO (Figure 4I, Table S2, p=0.002). Callus BV was decreased at 21 days post-fracture in both groups (Figure 4I, Table S2); however, these differences were not significantly different. Callus BV was further decreased in both groups at 28 and 35 days with no significant differences between groups. Total callus volume (TV) was highest in WT fractures at 14 days post-fracture, and significantly increased compared to Cx43cKO at this time (Figure 4J, Table S3, p=0.004). TV was not significantly different between WT and Cx43cKO at any other time-point. Bone volume over total volume (BV/TV) was not significantly different between WT and Cx43cKO fractures at any time between 14-35 days post-fracture, indicating that Cx43cKO fractures have concomitant decreases in both callus bone volume, and total callus volume. However, the proportion of

mineralized tissue in Cx43cKO fractures is not significantly different than WT fracture (Figure 4K, Table S4).

We used low-density BV as an indicator of bone remodeling. BV was measured at a low threshold (high and low density), and high threshold (high density). Low density BV was calculated by subtracting high-density BV from total BV. At 14 days post-fracture, peak low density BV was observed in both groups, with a significant increase in WT compared to Cx43cKO (Figure 4L, Table S5, p=0.0001). Changes in low-density BV were not significantly different between WT and Cx43cKO between 21 and 35 days, with a progressive decrease over time (Figure 4L, Table S5).

Cx43cKO fractures have decreased torsional rigidity

No significant changes in ultimate torque were observed between WT and Cx43cKO at any time-point, and ultimate torque was not significantly increased in WT or Cx43cKO from 14 to 35 days (Figure 5A, Table S6). In contrast, torsional rigidity was significantly increased in WT fractures compared to Cx43cKO at 21, 28, and 35 days post-fracture. Torsional rigidity was not different between WT and Cx43cKO at 14 days (p=0.92). Peak torsional rigidity occurred in both groups at 21 days post-fracture but was significantly increased in WT (p=0.0012), with a decrease at 28 days but remained significantly increased in WT (p=0.0195). By 35 days, torsional rigidity was still significantly increased in WT fractures compared to Cx43cKO (Figure 5B,Table S7, p=0.0011).

Discussion

In this study we have shown that Cx43 deficiency in mature osteoblasts and osteocytes results in decreased bone formation, remodeling, and biomechanical properties during fracture healing. To our knowledge this is the first study to identify an important role for Cx43 during fracture healing. Cx43cKO fractures heal with significant decreases in BV, less mineralization of the callus as assessed by histomorphometry, and decreased torsional rigidity between 21 and 35 days post-fracture. These data support our hypothesis that loss of Cx43 during fracture healing results in decreased osteoblast differentiation and bone formation, and is consistent with regulation of osteoblastic differentiation by Cx43 [3-5]. Stable transfection with Cx43 increases proliferation, and mineralization [2] as well as expression of osteocalcin and bone sialoprotein [3] in osteoblastic UMR 106 cells. Additionally, loss of Cx43 results in decreased alkaline phosphatase (AP) activity and osteocalcin expression in human fetal osteoblasts [5], and osteoblastic cells from Cx43 null mice display decreased differentiation and mineralization compared to those from WT mice [4]. Defects in both intramembranous and endochondral ossification are observed in Cx43 null mice [4], further indicating the requirement for Cx43 in osteoblast differentiation and mineralization.

In addition to bone formation, loss of Cx43 during fracture healing also alters bone resorption. Cortical bone at the fracture site remains un-resorbed in Cx43cKO fractures, while this bone is replaced by callus, and new bone formation in WT fractures. Cx43cKO fractures also have fewer TRAP+ osteoclasts in the callus between 14-28 days, indicative of decreased bone resorption. Cx43 is expressed in osteoclasts in areas of active bone resorption [25, 26] and inhibition of Cx43 expression and GJIC decreases osteoclast formation [19], degree of multi-nucleation [27] and activity [19, 28, 29], while abundant Cx43 expression is seen in the giant osteoclasts of Paget's disease [27], indicating the important role of Cx43 in regulating osteoclastogenesis. In this model of conditional Cx43 deficiency, only committed osteoblasts and osteocytes are affected, while expression of Cx43 should not be altered in osteoclasts. The decrease in TRAP+ osteoclasts in Cx43cKO fractures may be a result of the decreased bone formation observed in the Cx43cKO mice

(by histomorphometry at 14 and 28 days), and as such, decreased substrate for osteoclasts to resorb, resulting in a need for fewer osteoclasts. Interestingly, the significant decrease in the number of TRAP+ osteoclasts in the fracture callus of Cx43cKO mice is in contrast to the baseline phenotype of these mice. Recent work from our lab and others have shown an increased number of TRAP+ osteoclasts in Cx43cKO mice relative to WT [11, 30], while Watkins *et al* showed that increased osteoclastogenesis in Cx43cKO mice using the Dermo-1 Cre was the result of decreased *Osteoprotegerin* (*Opg*) production by Cx43 deficient osteoblasts [31]. We suspect this difference is due to the unique cellular milieu that accompanies fracture healing, with more immature osteoblasts and osteoblast precursors, as well as more active modeling/ remodeling compared to un-fractured bone.

In this genetic model of conditional Cx43 knockout, deletion of Cx43 does not occur until osteoblastic maturation enters the osteocalcin-expressing phase [21]. During fracture healing, periosteal progenitor cells migrate to the fracture site resulting in formation of a soft callus. These progenitor cells eventually differentiate to osteoblastic cells, which then mineralize the callus [32, 33]. Recent work by Ushiki and colleagues has shown that initial mineralization of the fracture callus is initiated by Collagen I expressing cells, with minimal contribution by osteocalcin^{+} cells [34]. This suggests that in our model, the majority of cells in the early healing stages have relatively normal Cx43 expression; although there is a population of resident osteocalcin+ cells at the bone surface that react to the fracture by altering their orientation [34]. Despite the modest contribution of osteocalcin^{+} cells, and thus the low degree of Cx43KO in the fracture callus, Cx43cKO fractures display delayed/ diminished healing as evidenced by decreased mechanical properties. This suggests that cells outside the fracture environment may play an integral role in mineralization and remodeling of the fracture. One possible candidate for this cell is the osteocyte. Cx43 can regulate osteocyte survival [35], and we have shown that Cx43 is expressed in cortical bone osteocytes during fracture healing. Osteocytes express both *Osteopontin* (*Opn*) [36], and members of the BMP signaling family [37] during fracture healing, suggesting an important role for osteocytes in mineralization of the fracture callus. Thus, osteocytic, more so than osteoblastic, Cx43 deficiency, may contribute to the changes in fracture healing we observed in Cx43cKO mice.

Cx43 may also play an important role in the chondrogenic phase of healing. Cx43 is expressed in the chondrocytes of the bridging callus, and a larger Alcian blue stained callus is observed in Cx43cKO fractures. While the role of Cx43 in chondrogenesis is not well understood, many studies have shown expression of Cx43 in mature chondrocytes [16-18], and during chondrogenic differentiation [38, 39]. Inhibition of GJIC, or a dominant-negative form of Cx43, leads to decreased chondrogenesis [38, 39] and impairs the condensation phase of differentiation [38]. These data suggest that loss of Cx43 during fracture healing could result in a smaller cartilaginous callus, however, in this study, Cx43cKO fractures actually have a larger Alcian blue stained callus compared to WT. One explanation for this is that we are using Osteocalcin-Cre, resulting in deletion of Cx43 in mature osteoblasts and osteocytes. Expression of Cx43 in chondrocytes is not likely to be affected in this model, and as such, chondrogenesis probably progresses normally; however, the transition to a mineralized callus, and replacement of the chondrocytes is impaired due to loss of Cx43 in osteoblasts, as shown by the persistence of Alcian blue staining in the cKO callus at 28 days. This persistence of cartilage may explain the decreased torsional rigidity at 28 days post-fracture observed in the Cx43cKO, while the WT callus has progressed to a more mineralized state at this time leading to improved biomechanics.

The decreased torsional rigidity, or stiffness, we observed in Cx43cKO mice suggests not only impaired healing, but also indicates a difference in callus composition. A callus composed of cartilage is less stiff than a more mineralized callus [40], and increased micro-

motion at the fracture site can delay consolidation and mineralization of the callus [41, 42]. At 14 days post-fracture, there was a significant increase in low-density bone volume in WT compared to Cx43cKO, suggestive of new woven bone formation. This is followed by histological observation of new islands of mineralized tissue and significant improvements in torsional rigidity compared to both WT fractures at 14 days, and Cx43cKO fractures at 14 and 21 days. These data indicate that early formation of low-density woven bone in WT mice may result in the enhanced biomechanics of WT fractures at 21-35 days compared to Cx43cKO fractures. We have chosen to use biomechanical torsion testing, rather than three-point bending, as torsion testing results in equal torque across all areas of the callus, while three-point bending results in un-equal forces across the callus, so failure may not occur at the weakest point of the fracture callus [43].

In summary, these studies identify a novel role for the gap junction protein Cx43 during fracture healing, suggesting that loss of Cx43 can result in decreased bone formation, and osteoclast activity. Therefore, enhancing Cx43 expression or GJIC may provide a novel means to enhance bone formation during fracture healing. Indeed, parathyroid hormone, which increases osteoblastic cell GJIC [44] also enhances fracture healing [20], supporting the concept that targeting connexins and GJIC will improve fracture healing.

Supplementary Material

Refer to Web version on PubMed Central for supplementary material.

Acknowledgments

This work was supported by NIH R01 AG13087.

References

1. Donahue HJ. Gap junctions and biophysical regulation of bone cell differentiation. Bone. 2000; 26(5):417–22. [PubMed: 10773579]
2. Gramsch B, et al. Enhancement of connexin 43 expression increases proliferation and differentiation of an osteoblast-like cell line. Exp Cell Res. 2001; 264(2):397–407. [PubMed: 11262196]
3. Lecanda F, et al. Gap junctional communication modulates gene expression in osteoblastic cells. Mol Biol Cell. 1998; 9(8):2249–58. [PubMed: 9693379]
4. Lecanda F, et al. Connexin43 deficiency causes delayed ossification, craniofacial abnormalities, and osteoblast dysfunction. J Cell Biol. 2000; 151(4):931–44. [PubMed: 11076975]
5. Li Z, et al. Modulation of connexin43 alters expression of osteoblastic differentiation markers. Am J Physiol Cell Physiol. 2006; 290(4):C1248–55. [PubMed: 16319124]
6. Plotkin LI, Manolagas SC, Bellido T. Transduction of cell survival signals by connexin-43 hemichannels. J Biol Chem. 2002; 277(10):8648–57. [PubMed: 11741942]
7. Saunders MM, et al. Gap junctions and fluid flow response in MC3T3-E1 cells. Am J Physiol Cell Physiol. 2001; 281(6):C1917–25. [PubMed: 11698250]
8. Saunders MM, et al. Fluid flow-induced prostaglandin E2 response of osteoblastic ROS 17/2.8 cells is gap junction-mediated and independent of cytosolic calcium. Bone. 2003; 32(4):350–6. [PubMed: 12689677]
9. Taylor AF, et al. Mechanically stimulated osteocytes regulate osteoblastic activity via gap junctions. Am J Physiol Cell Physiol. 2007; 292(1):C545–52. [PubMed: 16885390]
10. Grimston SK, et al. Attenuated response to in vivo mechanical loading in mice with conditional osteoblast ablation of the connexin43 gene (Gja1). J Bone Miner Res. 2008; 23(6):879–86. [PubMed: 18282131]
11. Zhang Y, et al. Enhanced osteoclastic resorption and responsiveness to mechanical load in gap junction deficient bone. PLoS One. 2011; 6(8):e23516. [PubMed: 21897843]

12. Meyer RA Jr. et al. Young, adult, and old rats have similar changes in mRNA expression of many skeletal genes after fracture despite delayed healing with age. J Orthop Res. 2006; 24(10):1933–44. [PubMed: 16894589]

13. Reaume AG, et al. Cardiac malformation in neonatal mice lacking connexin43. Science. 1995; 267(5205):1831–4. [PubMed: 7892609]

14. Chung DJ, et al. Low peak bone mass and attenuated anabolic response to parathyroid hormone in mice with an osteoblast-specific deletion of connexin43. J Cell Sci. 2006; 119(Pt 20):4187–98. [PubMed: 16984976]

15. Schindeler A, et al. Bone remodeling during fracture repair: The cellular picture. Semin Cell Dev Biol. 2008; 19(5):459–66. [PubMed: 18692584]

16. Donahue HJ, et al. Chondrocytes isolated from mature articular cartilage retain the capacity to form functional gap junctions. J Bone Miner Res. 1995; 10(9):1359–64. [PubMed: 7502708]

17. Tonon R, D'Andrea P. Interleukin-1beta increases the functional expression of connexin 43 in articular chondrocytes: evidence for a Ca2+-dependent mechanism. J Bone Miner Res. 2000; 15(9):1669–77. [PubMed: 10976987]

18. Tonon R, D'Andrea P. The functional expression of connexin 43 in articular chondrocytes is increased by interleukin 1beta: evidence for a Ca2+-dependent mechanism. Biorheology. 2002; 39(1-2):153–60. [PubMed: 12082278]

19. Ransjo M, Sahli J, Lie A. Expression of connexin 43 mRNA in microisolated murine osteoclasts and regulation of bone resorption in vitro by gap junction inhibitors. Biochem Biophys Res Commun. 2003; 303(4):1179–85. [PubMed: 12684060]

20. Alkhiary YM, et al. Enhancement of experimental fracture-healing by systemic administration of recombinant human parathyroid hormone (PTH 1-34). J Bone Joint Surg Am. 2005; 87(4):731–41. [PubMed: 15805200]

21. Zhang M, et al. Osteoblast-specific knockout of the insulin-like growth factor (IGF) receptor gene reveals an essential role of IGF signaling in bone matrix mineralization. J Biol Chem. 2002; 277(46):44005–12. [PubMed: 12215457]

22. Castro CH, et al. Development of mice with osteoblast-specific connexin43 gene deletion. Cell Commun Adhes. 2003; 10(4-6):445–50. [PubMed: 14681055]

23. Bonnarens F, Einhorn TA. Production of a standard closed fracture in laboratory animal bone. J Orthop Res. 1984; 2(1):97–101. [PubMed: 6491805]

24. Erlebacher A, Derynck R. Increased expression of TGF-beta 2 in osteoblasts results in an osteoporosis-like phenotype. J Cell Biol. 1996; 132(1-2):195–210. [PubMed: 8567723]

25. Jones SJ, et al. The incidence and size of gap junctions between the bone cells in rat calvaria. Anat Embryol (Berl). 1993; 187(4):343–52. [PubMed: 8390141]

26. Su M, et al. Expression of connexin 43 in rat mandibular bone and periodontal ligament (PDL) cells during experimental tooth movement. J Dent Res. 1997; 76(7):1357–66. [PubMed: 9207768]

27. Schilling AF, et al. Gap junctional communication in human osteoclasts in vitro and in vivo. J Cell Mol Med. 2008; 12(6A):2497–504. [PubMed: 18266960]

28. Ilvesaro J, Tavi P, Tuukkanen J. Connexin-mimetic peptide Gap 27 decreases osteoclastic activity. BMC Musculoskelet Disord. 2001; 2:10. [PubMed: 11747476]

29. Ilvesaro J, Vaananen K, Tuukkanen J. Bone-resorbing osteoclasts contain gap-junctional connexin-43. J Bone Miner Res. 2000; 15(5):919–26. [PubMed: 10804022]

30. Bivi N, et al. Cell Autonomous Requirement of Connexin 43 for Osteocyte Survival: Consequences for Endocortical Resorption and Perisoteal Bone Formation. J Bone Miner Res. 2012; 27(2):374–389. [PubMed: 22028311]

31. Watkins M, et al. Osteoblast connexin43 modulates skeletal architecture by regulating both arms of bone remodeling. Mol Biol Cell. 2011; 22(8):1240–51. [PubMed: 21346198]

32. Einhorn TA. The cell and molecular biology of fracture healing. Clin Orthop Relat Res. 1998; (355 Suppl):S7–21. [PubMed: 9917622]

33. Ozaki A, et al. Role of fracture hematoma and periosteum during fracture healing in rats: interaction of fracture hematoma and the periosteum in the initial step of the healing process. J Orthop Sci. 2000; 5(1):64–70. [PubMed: 10664441]

34. Ushiku C, et al. Long bone fracture repair in mice harboring GFP reporters for cells within the osteoblastic lineage. J Orthop Res. 2010; 28(10):1338–47. [PubMed: 20839319]
35. Bivi N, et al. Cell autonomous requirement of connexin 43 for osteocyte survival: consequences for endocortical resorption and periosteal bone formation. J Bone Miner Res. 2011
36. Hirakawa K, et al. Localization of the mRNA for bone matrix proteins during fracture healing as determined by in situ hybridization. J Bone Miner Res. 1994; 9(10):1551–7. [PubMed: 7817800]
37. Yu YY, et al. Immunolocalization of BMPs, BMP antagonists, receptors, and effectors during fracture repair. Bone. 2010; 46(3):841–51. [PubMed: 19913648]
38. Loty S, et al. Association of enhanced expression of gap junctions with in vitro chondrogenic differentiation of rat nasal septal cartilage-released cells following their dedifferentiation and redifferentiation. Arch Oral Biol. 2000; 45(10):843–56. [PubMed: 10973558]
39. Zhang W, Green C, Stott NS. Bone morphogenetic protein-2 modulation of chondrogenic differentiation in vitro involves gap junction-mediated intercellular communication. J Cell Physiol. 2002; 193(2):233–43. [PubMed: 12385001]
40. White AA 3rd, Panjabi MM, Southwick WO. The four biomechanical stages of fracture repair. J Bone Joint Surg Am. 1977; 59(2):188–92. [PubMed: 845202]
41. Augat P, et al. Quantitative assessment of experimental fracture repair by peripheral computed tomography. Calcif Tissue Int. 1997; 60(2):194–9. [PubMed: 9056170]
42. Probst A, et al. Callus formation and fixation rigidity: a fracture model in rats. J Orthop Res. 1999; 17(2):256–60. [PubMed: 10221843]
43. Morgan, EF.; Einhorn, TA.; Asbmr. Biomechanics of Fracture Healing, in Primer on the Metabolic Bone Diseases and Disorders of Mineral Metabolism. John Wiley & Sons, Inc.; 2009. Chapter 12; p. 65-69.
44. Donahue HJ, et al. Cell-to-cell communication in osteoblastic networks: cell line-dependent hormonal regulation of gap junction function. J Bone Miner Res. 1995; 10(6):881–9. [PubMed: 7572312]

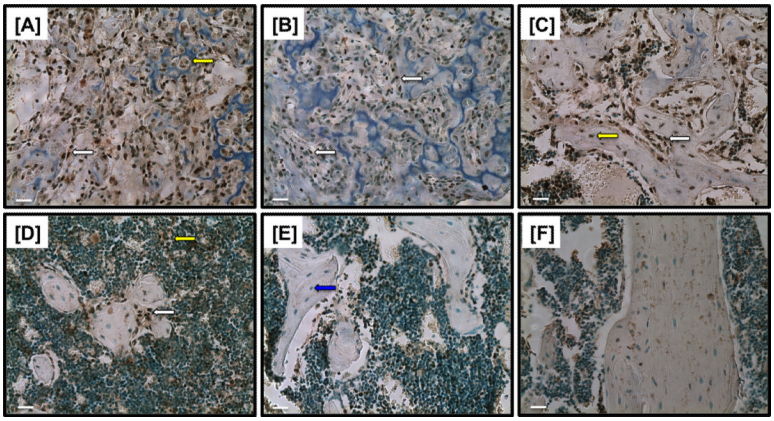

Figure 1.

Immunohistochemical staining of Cx43 at [A] 10, [B] 14, [C] 21, [D] 28, [E] 35 days post-fracture. Cx43 expression occurs in osteoblasts lining new bone formation (white arrows [A-D]), and in osteocytes (yellow arrows [C]), in chondrocytes of the callus (yellow arrow [A]), and in marrow cells (yellow arrow [D]). A lack of Cx43 staining is observed in osteocytes/osteoblasts at 35 days post-fracture (blue arrow [E]). [F] Non-immune IgG control shows a lack of Cx43 expression. 20X magnification. Scale bars represent 100 microns.

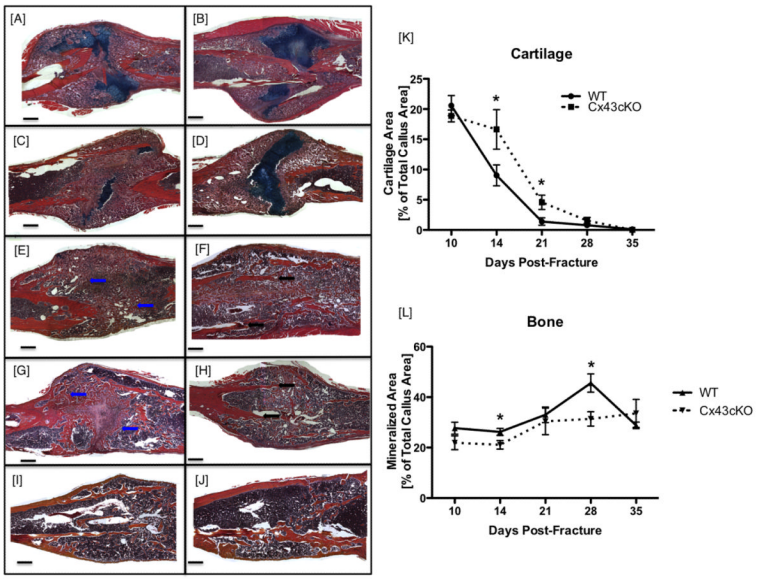

Figure 2.

Histology and histomorphometry of WT [A, C, E, G, I], and Cx43cKO [B, D, F, H, J] fractures at [A&B] 10, [C&D] 14, [E&F] 21, [G&H] 28, and [I&J] 35 days post-fracture respectively. Sections were stained with Alcian Blue Hematoxylin/ Orange G. Cx43cKO fractures have larger areas of Alcian blue stained cartilage at 14 days [D&K]. Increased areas of new woven bone formation are apparent in the WT callus at 21 and 28 days (blue arrows, [E, G]). Cortical bone is not resorbed in Cx43cKO fractures (black arrows, [F, H]). 4x magnification. Scale bars represent 400 microns. [K&L] Histomorphometry of [K] cartilage, and [L] mineralized tissue as a proportion of total callus area from 10-35 days post-fracture. Data are presented as ± SEM, n=3/group, *=$p<0.05$.

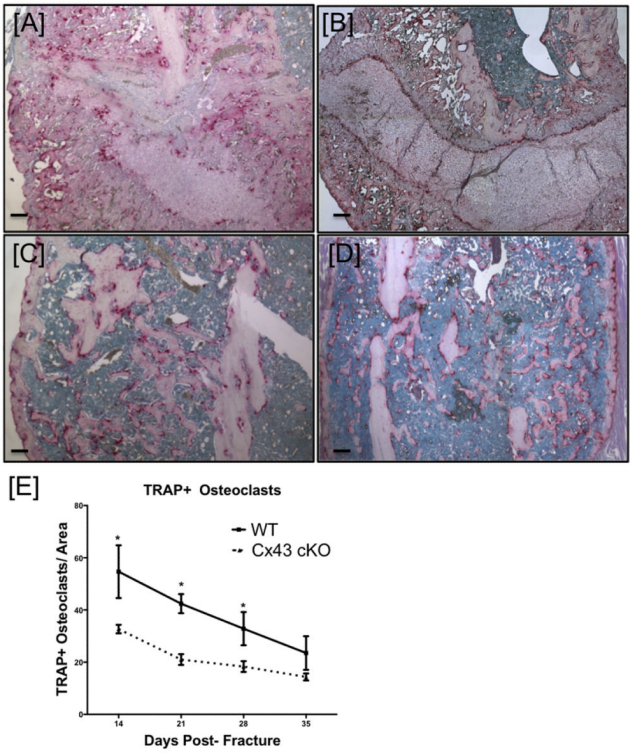

Figure 3.

[A-D] Representative images of TRAP staining of osteoclasts in WT [A, C] and Cx43cKO [B, D] fractures at 14 [A, B] and 21 [C, D] days post-fracture. [E] Quantification of TRAP+ osteoclasts. Data are presented ± SEM, n=3, *$p<0.05$. TRAP+ osteoclasts were counted for three sections/specimen, with three specimens/group/time-point. Scale bars represent 100 microns.

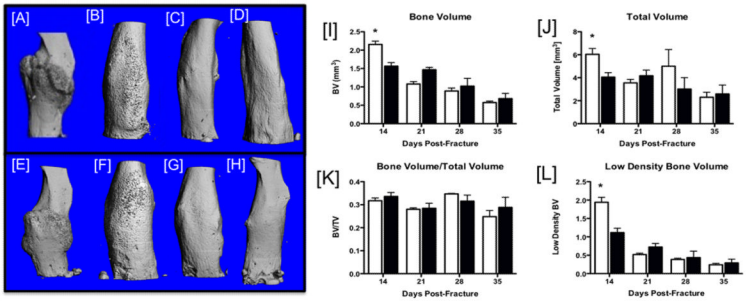

Figure 4.

[A-H] Representative three-dimensional reconstructions of microCT scans of WT [A-D] and Cx43cKO [E-H] fractures at [A, E] 14, [B, F] 21, [C, G] 28, and [D, H] 35 days post-fracture. [I-L]: Quantification of callus mineralization during fracture healing in WT (white bars) and Cx43cKO (black bars). [I] Total callus bone volume (BV), [J] Total callus volume (TV), [K] BV/TV, [L] Low-density bone volume. Data are presented ±SEM, N=8-12/group, *=$p<0.05$.

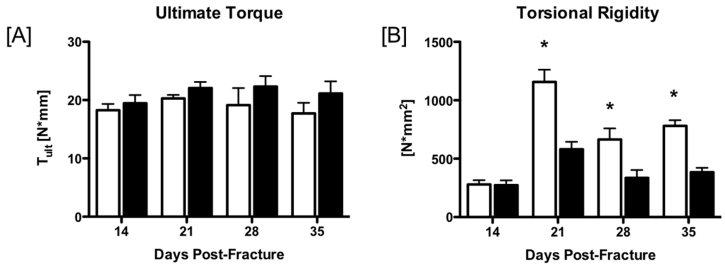

Figure 5.

[A] Ultimate Torque (T_{ult}) at failure of WT (white bars) and Cx43cKO fractures (black bars) from 14-35 days post-fracture. [B] Torsional Rigidity. Data are presented ±SEM, N=8-12/ group, *=$p<0.05$.